EM Radiation Analysis of Electrical Dipole in Close Vicinity of Dissipative Object

Juraj Bartolic, Zvonimir Sipus, Sinisa Skokic, Tomislav Debogovic
Department of Wireless Communications
Faculty of Electrical Engineering and Computing
University of Zagreb, Zagreb, Croatia
e-mail: Juraj.Bartolic@fer.hr

Davor Crnogorac
Ericsson Nikola Tesla
Zagreb, Croatia

Abstract— **A phenomenon of electromagnetic wave propagation produced by a GSM mobile phone antenna at the operating frequency 950 MHz, placed in close vicinity of a dissipative object has been investigated and measured. The model (phantom head) of a dissipative object representing and simulating electromagnetic properties of human head tissue in the GSM frequency band has been made. Dielectric properties of the phantom head have been measured. A GSM mobile phone antenna and GSM base station antenna were approximated with dipole antennas and adjusted to GSM frequency band. Radiation patterns and antenna efficiency of the GSM mobile phone antenna settled near the phantom head for vertical and horizontal polarization of the antennas have been measured and recorded on three specific frequencies inside the GSM frequency band.**

Keywords- mobile communications; antenna; phantom head; antenna efficiency

I. Introduction

When studying interaction between electro-magnetic fields and biological subjects as the human head is, it is not possible to measure directly and harmlessly dissipative properties of the human head during the GSM communication and its influence on the radiation patterns and efficiency of GSM mobile phone antenna.

Some of the previous measurements included computer modeling of the human head [1] along with FDTD methodology derived from Maxwell's time-domain equations [2] in order to indirectly measure the specific absorption rate (SAR) distribution of the EM energy that was dissipated in the human head during the simulated GSM communication, including the influence of the human head and handset model on the gain, efficiency and radiation pattern of the GSM mobile phone antenna.

Proposed investigation was motivated by the need for an efficient and fast method of determining mobile antenna efficiency in vicinity of the human body. In order to preserve human health or live organism in general when measuring EM radiation and effects, we made a phantom head – a liquid mixture that represents dielectric properties of the real human head tissue. Among quite different antenna types employed in modern mobile phones and terminals [3-6], we chose a simple half wavelength dipole antenna.

The main goal of this experimental and theoretical investigation is to observe the interaction of the human head with GSM mobile phone antenna, and the influence of the human head to the radiation patterns and radiation efficiency of the antenna. In that sense we also developed a measurement setup for simple and efficient measurements antenna measurements.

II. Phisical model of the human head

The dielectric properties of the tissue with a great volume percentage of water (for e.g. muscle tissue and most of the organ tissues in the human body and head), in the frequency band from 1 MHz to 2 GHz are mostly defined by the dielectric properties and amount of water and salts dissolved in the tissue. These organs and tissues rich with water have relatively high values of the conductivity and permittivity ($\varepsilon_r \approx 50$, $\sigma \approx 1$ S/m), which results in a pretty high reflection and attenuation of the incident EM wave (approx. 230 dB/m).

Liquid mixture (phantom of the human head tissue) for GSM frequency band, used in this research, was made according to the instructions in [7] and [8]. For liquid phantoms, the electric permittivity is controlled by adding proper amount of consumable sugar because sugar has very low specific permittivity (see TABLE I). For controlling electric conductivity of the phantom, sodium chloride (NaCl) is used in all cases.

TABLE I

Ingredients for the phantom head

Ingredients	**Net mass**
distilled water	2.00 kg
sugar (crystal consumable white)	2.89 kg
consumable salt (NaCl)	34.45 g
TOTAL	4.92 kg

The right amounts of ingredients for the phantom used in the measurements were calculated from [8].

The phantom is made and measured at the constant room temperature (22° C) in order to make measured dielectric properties more similar to the properties of the real tissue close to the body temperature.

A. Measurement of Phantom Properties

Measuring dielectric properties of the phantom was performed according to non-destructive in vivo method developed by Mosig [9]. The measurement setup consisted of a coaxial probe and the network analyzer that measures reflection parameters on the probe connector. The probe itself is a 50 Ω open-ended semi-rigid coaxial cable filled with the teflon dielectric. The reflection coefficient is measured with the HP 8720B network analyzer calibrated via standard calibration procedure with three known loads at the plane of the probe connector. However, an error box appears between the probe connector plane and probe open-end plane [4]. In order to take into account this error box, three additional reflection coefficient measurements of known loads are necessary: open end, short circuit and distilled water (the dielectric constant of distilled water, as a function of frequency and temperature, is well known [5]). With these measurements the s parameters of the error box are determined.

$$S_{11} = \frac{\Gamma_{OE}\Gamma_{SC}s_3(s_1 - s_2) + \Gamma_{SC}\Gamma_{H_2O}s_1(s_2 - s_3) + \Gamma_{OE}\Gamma_{H_2O}s_2(s_3 - s_1)}{\Gamma_{OE}\Gamma_{SC}(s_1 - s_2) + \Gamma_{SC}\Gamma_{H_2O}(s_2 - s_3) + \Gamma_{OE}\Gamma_{H_2O}(s_3 - s_1)}, \quad (1)$$

$$S_{22} = \frac{\Gamma_{H_2O}(s_2 - S_{11}) - \Gamma_{SC}(s_3 - S_{11})}{\Gamma_{SC}\Gamma_{H_2O}(s_2 - s_3)}, \quad (2)$$

$$S_{12}S_{21} = S_{21}^2 \frac{(S_{11} - s_2) + (1 - S_{22}\Gamma_{SC})}{\Gamma_{SC}}, \quad (3)$$

where s_1, s_2, and s_3 are the measured reflection coefficients of three known loads with the true reflection coefficients Γ_{OE}, Γ_{SC} and Γ_{H2O}, respectively. The true reflection coefficient Γ_P of the phantom is then related to the measured reflection coefficient Γ_M as follows:

$$\Gamma_P = \frac{\Gamma_M - S_{11}}{S_{22}\Gamma_M + S_{12}S_{21} - S_{11}S_{22}}. \quad (4)$$

Permittivity ε_r of the tested phantom can be directly calculated from the reflection coefficient Γ_P as a function of frequency (ω) by a relation:

$$\varepsilon_r = \frac{-2}{\omega C_0 Z_0} \cdot \frac{|\Gamma_P|\sin[\arg(\Gamma_P)]}{1 + 2|\Gamma_P|\cos[\arg(\Gamma_P)] + |\Gamma_P|^2} - \frac{C_f}{C_0}, \quad (5)$$

where C_0 = 0.022 pF and C_f = 0.001 pF represent characteristic capacitances of the probe at the room temperature (22ºC), and Z_0 = 50Ω is characteristic impedance of the coaxial line.

Electric conductivity (σ) of the phantom is represented with the following formula:

$$\sigma = \frac{\varepsilon_0}{C_0 Z_0} \cdot \frac{1 - |\Gamma_P|^2}{1 + 2|\Gamma_P|\cos[\arg(\Gamma_P)] + |\Gamma_P|^2}, \quad (6)$$

which is a function of frequency, although the frequency dependence is not explicitly visible (the Γ_P coefficient is, in fact, a function of frequency).

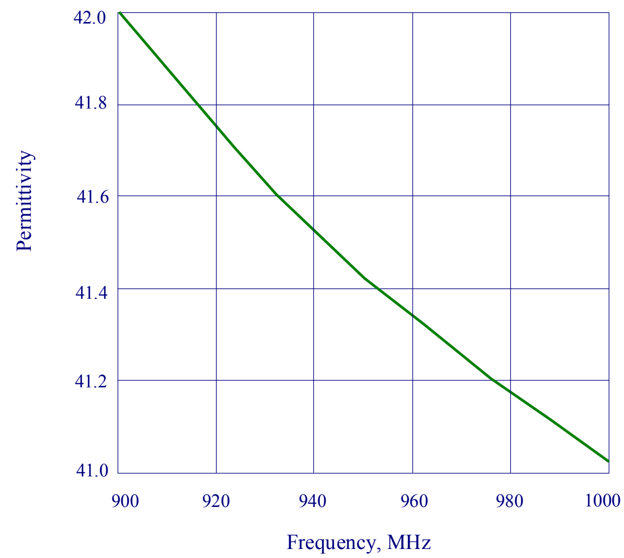

Figure 1. Phantom permittivity as a function of frequency

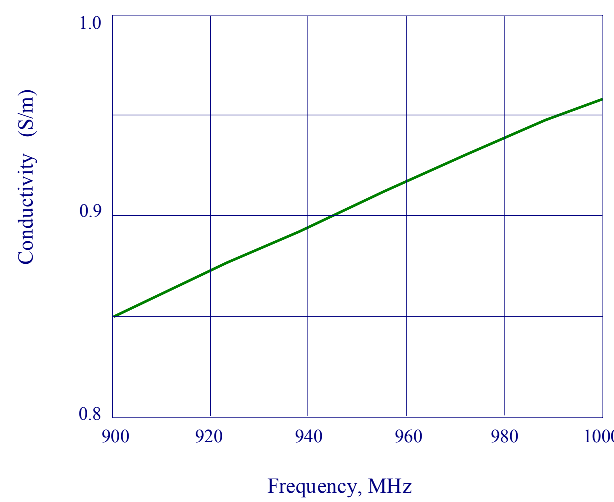

Figure 2. Phantom conductivity as a function of frequency

Permittivity ε_r and electric conductivity σ of the tested phantom can be directly calculated from the reflection coefficient Γ_P as a function of frequency. All the measurements are performed in the frequency range from 900 to 1000 MHz. Figs. 1 and 2 show the measured permittivity and electric conductivity of the phantom. It is seen that the value of the phantom head permittivity slowly decreases as the frequency increases, while the value of the electric conductivity is slowly increasing with frequency. At the GSM frequencies, all measured results correspond very well with the previous results [9,10].

III. Radiation Patterns of an Electric Dipole Close to the Phantom Head

The *E*- and *H*-plane radiation patterns of an electric half-wave dipole that simulated the real GSM mobile phone antenna, near the phantom head have been observed and recorded.

The measurement setup, shown in Fig. 3, consists of two identical half-wave dipole antennas, a dissipative object (the phantom head) seating on a turntable close to the transmitting antenna, network analyzer, and a PC for data processing. Two half-wave dipole antennas are designed and manufactured in our laboratory for the GSM frequency band. A cylindrical shape of the phantom is chosen because we intended to make a comparison with the simulated results from the software package CyMPA developed in our laboratory, which uses MoM in spectral domain [11]. Transmission parameters are corrected using return loss data via S_{11} and S_{22}. The influence of the reflections from the nearby objects is reduced using time domain reflectometer option of the network analyzer.

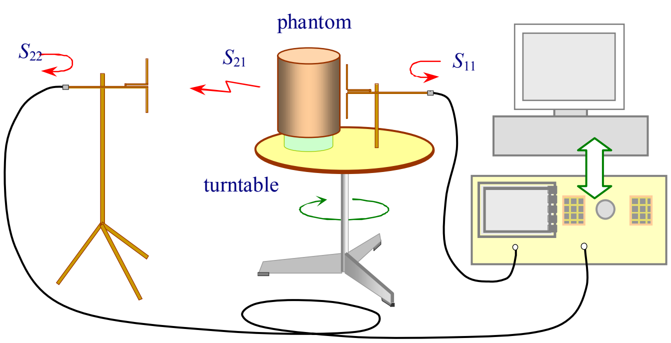

Figure 3. Radiation pattern measurement setup

The measurements were performed in the frequency range from 900 to 1000 MHz for the phantom spacing 0, 1, 2 and 5 cm from the receiving antenna. The measurement procedure explained above was performed for vertically and horizontally polarized antennas, which makes different radiation patterns shown in Figs. 4-9.

Figs. 4 and 5 show that the *H*-plane radiation pattern of the vertically polarized antenna at 950 MHz frequency is closer to the cardioid as the distance between the antenna and the phantom is gradually increasing. For the horizontally polarized dipole, radiation patterns show similar effects. It is obvious that the presence of the phantom splits the back lobe into three smaller separated back lobes and for the distance between the transmitting antenna and the phantom greater than 2 cm, the 'front' lobe is somewhat increased probably due to reflection phenomena at the phantom.

Radiation patterns in the *E*-plain are narrower as shown in Figs. 6 and 7. Maximal radiated power for the phantom spacing of 5 cm is greater than that for the dipole alone. This should be prescribed to the effect of the phantom as an reflector in that configuration.

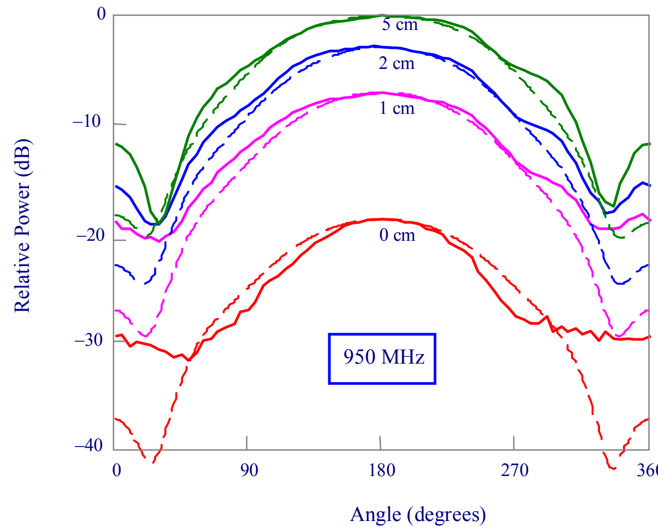

Figure 4. A comparison between 950 MHz measurements and a theoretical prediction of the *H*-plane radiation patterns for a dipole parallel to the phantom axis

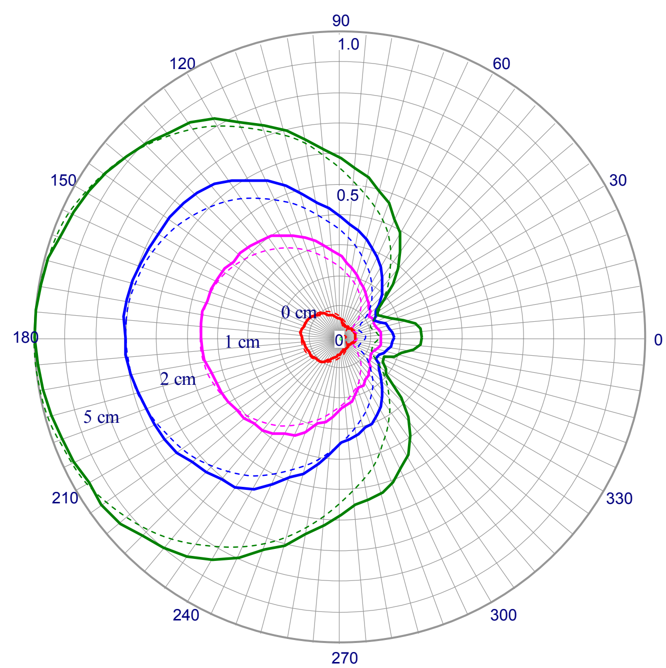

Figure 5. A comparison between measurements and a theoretical prediction of the *H*-plane radiation patterns for a dipole parallel to the phantom axis (polar plot at 950 MHz)

By using an extrapolation technique, a simple 3D radiation pattern was constructed do determine the dipole antenna efficiency in the presence of the human head phantom. The 3D radiation pattern was extrapolated using a simple formula

$$F(\theta,\varphi) = F_H(\theta)\sin^2\varphi + F_E(\theta)\cos^2(\varphi), \tag{7}$$

where $F_H(\theta)$ and $F_E(\theta)$ are 2D radiation patterns in two orthogonal planes.

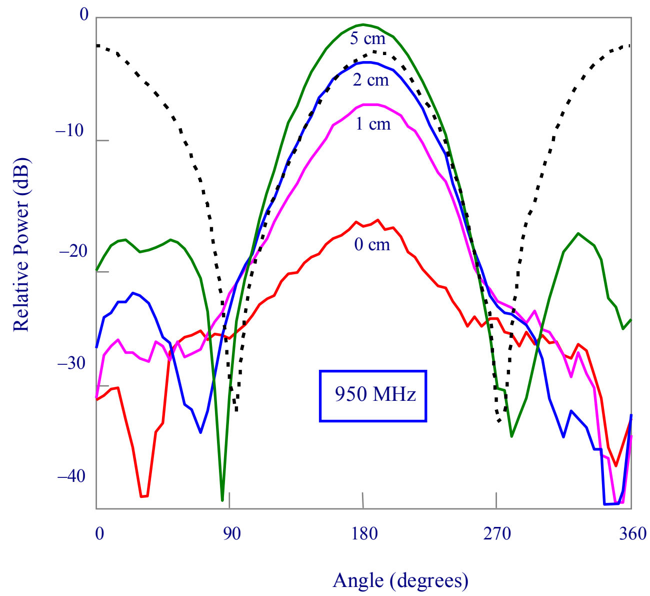

Figure 6. A comparison between measurements and a theoretical prediction of the *E*-plane radiation patterns for a dipole parallel to the phantom axis; the dotted line corresponds to the case without phantom

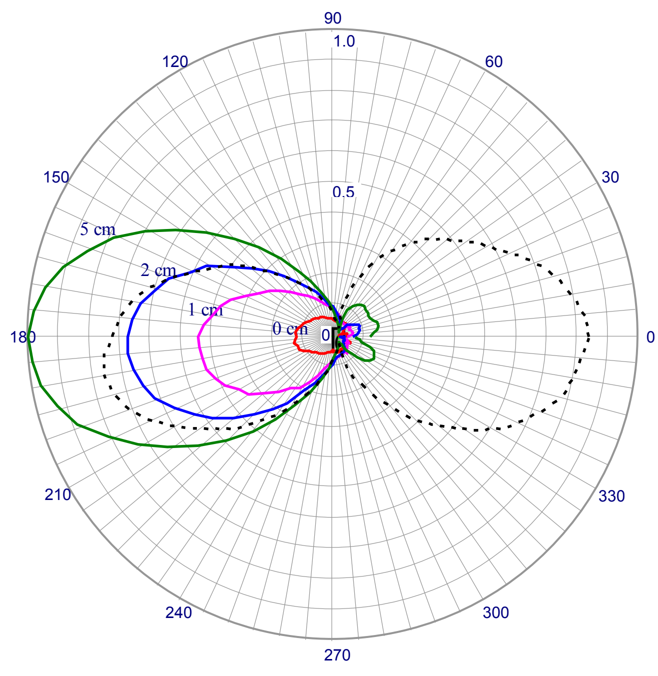

Figure 7. A comparison between measurements and a theoretical prediction of the *E*-plane radiation patterns for a dipole parallel to the phantom axis (polar plot at 950 MHz); the dotted line corresponds to the case without phantom

These radiation pattern measurements suggest substantial absorption of the electromagnetic energy into the phantom head. The absorption becomes greater as the distance between antenna and the phantom decreases. When the antenna is closest to the phantom (0 cm, the thinnest line on the diagrams), the EM absorption of the phantom increases, and takes value of less than 59% of the total radiated power for the horizontally polarized dipole and less than 42% for the vertically polarized dipole.

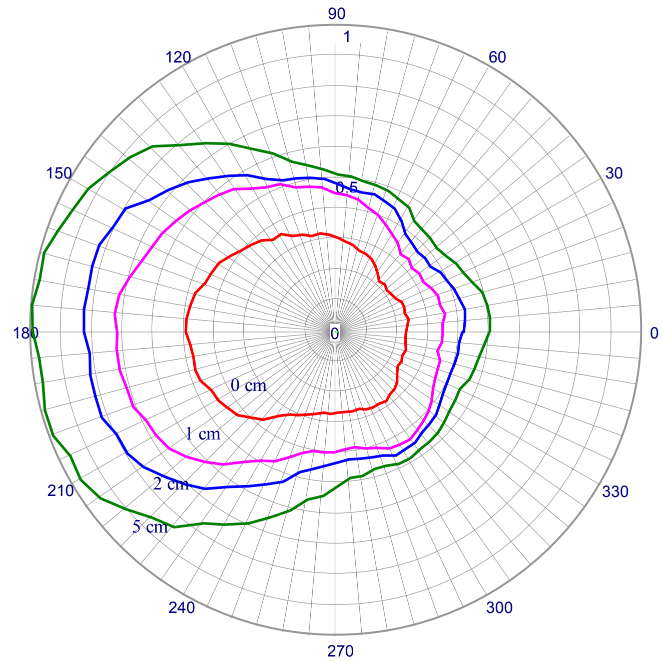

Figure 8. A comparison between measurements and a theoretical prediction of the *E*-plane radiation patterns for a dipole perpendicular to the phantom axis (polar plot at 950 MHz)

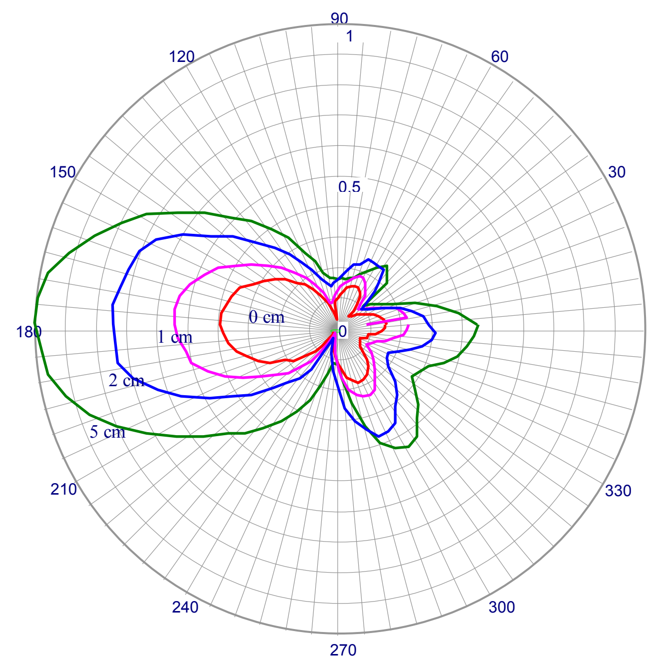

Figure 9. A comparison between measurements and a theoretical prediction of the *H*-plane radiation patterns for a dipole perpendicular to the phantom axis (polar plot at 950 MHz)

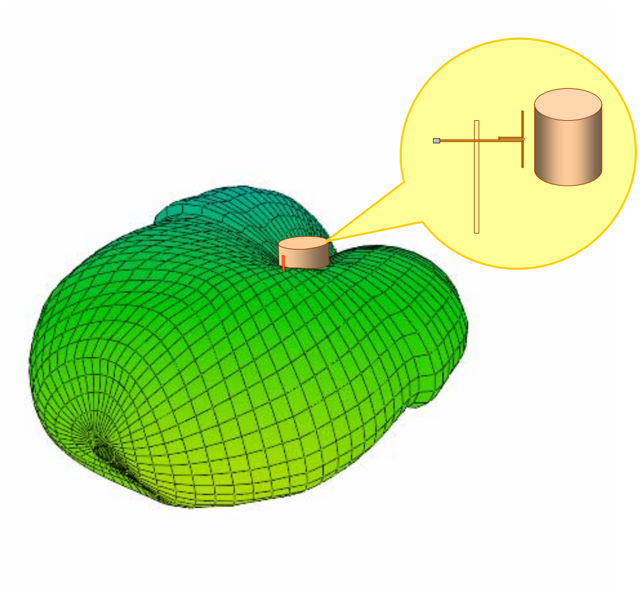

Figure 10. Extrapolated 3D radiation pattern of a dipole parallel to the phantom axis at 950 MHz

IV. Conclusions

The performances of an antenna placed in the proximity of a human head model have been investigated. A simplified experimental analysis of the EM radiation of the half-wave electrical dipole close to the phantom head in the GSM frequency band has been used. Measurements of the radiation pattern have been provided in two orthogonal planes. Based on a simple extrapolation formula, the radiation efficiency of a half-wave dipole antenna in presence of the human head phantom has been calculated from the radiation patterns measured in the *E*- and *H*-planes. Very good agreement between theoretical and experimental results has been found.

References

[1] K. Meksamoot, M. Krairiksh, J. Takada, "A Polarization Diversity PIFA on Portable Telephone and the Human Body Effects on Its Performance", IEICE Trans. Communications, vol. E84-B, No.9, September 2001.

[2] M. A. Jensen, Y. Rahmat-Samii, "EM Interaction of Handset Antennas and a Human in Personal Communications", Proceedings of the IEEE, vol. 83, No.1, January 1995.

[3] M. Martinez-Vazquez, "ACE 2 Activities on Small Terminal Technologies and Applications", Proceedings of the European Conference on Antennas and Propagation: EuCAP 2006, Paper No. 382926; pp. 1-4, Nice, France, 6-10 Nov. 2006.

[4] J. Bartolic, M. Knezevic, T. Debogovic, "Ultra Wideband Antenna of Two Bow-Tie Unipoles", Proceedings of the European Conference on Antennas and Propagation: EuCAP 2006, Paper No. 363977; pp. 1-4, Nice, France, 6-10 Nov. 2006.

[5] D. Bonefacic, J. Bartolic, D. Kocen, "Stacked Shorted Patch Antenna with Tilted Parasitic Radiator", Electronics Letters IEE, Vol. 37, pp. 1109-1110, 30th Aug. 2001.

[6] R. Zentner, Z. Sipus, J. Bartolic, "Optimization Synthesis of Broadband Circularly Polarized Microstrip Antennas by Hybrid Genetic Algorithm", Microwave and Optical Technology Letters, Vol. 14, pp. 197-201, Nov. 5, 2001.

[7] Z. Sipus, S. Skokic, J. Bartolic, "Measurements of Electromagnetic Parameters of Soil", Proceedings of the 17th International Conference on Applied Electromagnetics, (ICECom 2003), pp. 56-59, Dubrovnik 1-3 October 2003.

[8] R. Serrano Calvo, "Study of Losses due to Head and Hand of Mobile Phones with External and Built-in Antennas in Rever-beration Chamber", Master Thesis, Chalmers University of Technology, Gothenburg, 2001.

[9] J. R. Mosig, J. E. Besson, M. Gex-Fabry, F. E. Gardiol, "Reflection of an Open-Ended Coaxial Line and Application to Non-destructive Measurement of Materials", IEEE Trans. Instrumentation and Measurements, vol. IM-30, pp. 46–51, March 1981.

[10] K. W. Chan, "Microwave phantoms", COST 244: Biomedical Effects of Electromagnetic fields, Roma, 1994.

[11] S. Raffaelli, Z. Sipus, P-S Kildal, "Analysis and Measurements of Conformal Patch Array Antennas on Multilayer Circular Cylinder", IEEE Trans. on Antennas and Propagation, vol. 55, pp. 1105-1113, No. 3, 2005.